# Applications of the magnetic field line topology in space plasmas Part I: Introduction and theory

Bogdan Hnat[1], S. C. Chapman[1], N. W. Watkins[1,2], C. Liptrott[1], K. Shaji[1]

[1] CFSA, Physics Department, University of Warwick, Coventry, CV4 7AL, UK.
[2] Grantham Research Institute on Climate Change and the Environment, LSE, London, WC2A 2AE, UK

# Part I: Introduction and theory

- Magnetic field lines and topology
- Magnetic field properties
- Lagrangian versus Eulerian description of the field line
- Magnetic field line topology and the role of magnetic field gradient tensor
- Topological invariants of the magnetic field gradient tensor

# Magnetic field lines [1]

- **Magnetic field lines**: solutions of a differential equation at point $\mathbf{x}$

$$\boxed{d\mathbf{x}\times\mathbf{B}=0 \text{ or } B dx_i = B_i ds}$$

- **Example**: **2D x-point: B = (x, -y, 0)**

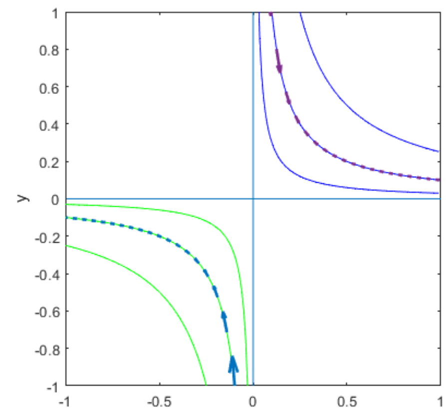


$$\frac{dx}{B_x}=\frac{dy}{B_y}\Rightarrow\frac{dx}{x}=-\frac{dy}{y}$$

$$\ln|x|=\ln\left|Ky^{-1}\right|\Rightarrow xy=K=const$$

- **Example**: **3D x-point: B = (x, -y, l)**

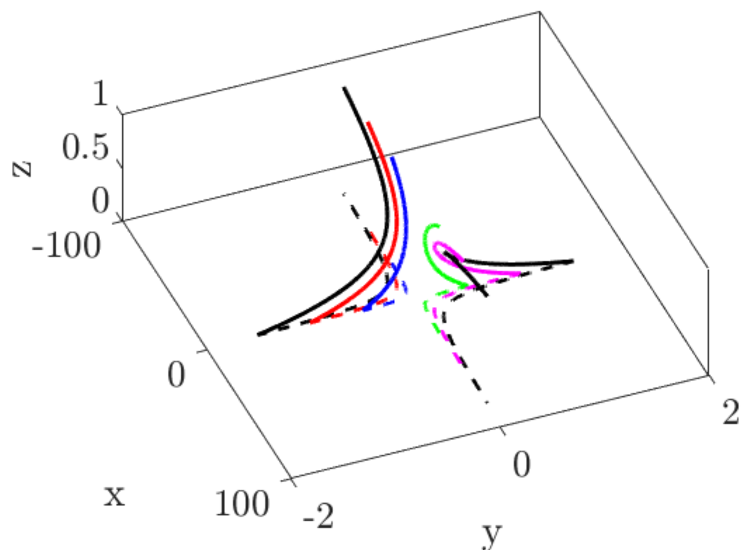


$$\frac{dx}{B_x}=\frac{dy}{B_y}=\frac{dz}{B_z}\Rightarrow\frac{dx}{x}=-\frac{dy}{y}=\frac{dz}{l}$$

$$x=X_0\exp(z/l),\quad y=Y_0\exp(-z/l)$$


**[1]** Priest and Démoulin, JGR 100 (1995)

# Magnetic field line topology [1, 2]

- A set of field lines viewed with respect to their mutual position, their links and their orientation in space [2].

- These properties are not affected by smooth deformations of lines.

- Two magnetic configurations are topologically equivalent if there is a continues deformation that vanishes at the boundaries which smoothly deforms one configuration into another [1].

- We will distinguish between the local and the global topology. Global topology can change due to changes at the boundaries or by a local process such as reconnection.

- I will refer to both local and global topology in the intro, but only local topology can be reconstructed from spacecraft observations.

**[2]** Hornig & Schindler, Physics of Plasmas 3, 781 (1996)

# Magnetic field properties

Consider time independent magnetic field vector $\mathbf{B}(\mathbf{x})$. **The most basic property that constrains its topology** is that for any closed surface $S$ with the outward normal vector $\mathbf{n}$

$$\boxed{\int_S \mathbf{B}\cdot\mathbf{n}\,dS = 0 \text{ or } \nabla\cdot\mathbf{B} = 0}$$

This implies existence of the **vector potential** $\mathbf{A}(\mathbf{x})$ such that:

$$\nabla\cdot\mathbf{B} = 0 \Rightarrow \mathbf{B} = \nabla\times\mathbf{A} \text{ and } \nabla\cdot\mathbf{A} = 0$$

Consider now an open surface $S$ with normal $\mathbf{n}$ enclosed by a contour $C$. **The magnetic flux through *S*** is

$$\boxed{\Phi = \int_S \mathbf{B}\cdot\mathbf{n}\,dS = \oint_C \mathbf{A}\cdot d\mathbf{x}}$$

In space magnetic field is often embedded into a complex plasma flow. We would like to understand how the field lines are affected by it.

# Lagrangian representation [3]

We **follow a parcel of plasma along its material line,** from a starting point **a** at time $t = 0$ to an arbitrary position **x** at time $t$. Now, **a** is an independent variable, while **x** is a dependent variable.

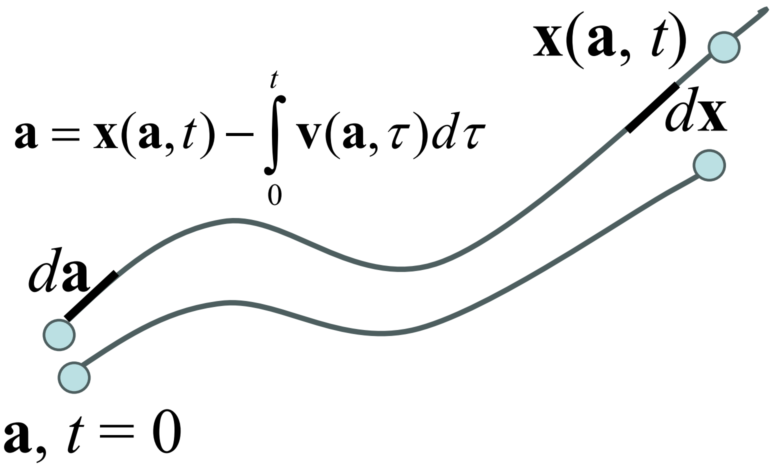


Lagrangian velocity field vector at **x**:

$$\mathbf{v}^L(\mathbf{a},t) = \mathbf{v}(\mathbf{x}(\mathbf{a},t),t)$$

Lagrangian (material) time derivative:

$$\boxed{\frac{D}{Dt} = \left(\frac{\partial}{\partial t}\right)_{\mathbf{a}} = \left(\frac{\partial}{\partial t}\right)_{\mathbf{x}} + \mathbf{v}\cdot\nabla} \text{ where } \mathbf{v} = \left(\frac{\partial \mathbf{x}}{\partial t}\right)_{\mathbf{a}}$$

An infinitesimal increment along the streamline for a fixed time $t$ (mind Einstein's summation convention)

$$\boxed{dx_i(a_j,t) = \frac{\partial x_i}{\partial a_j} da_j \quad \Rightarrow \quad \frac{D(d\mathbf{x})}{Dt} = (d\mathbf{x}\cdot\nabla)\mathbf{v}}$$


**[3]** H. K. Moffat Magnetic Field Generation in Electrically Conducting Fluids. Cambridge University Press, 1978

# Frozen-in magnetic field lines

In perfectly conducting plasma on MHD scales the induction equation is

$$\partial_t \mathbf{B} = \nabla \times \left( \mathbf{v} \times \mathbf{B} \right) = \mathbf{B} \cdot \nabla \mathbf{v} - \mathbf{B}(\nabla \cdot \mathbf{v}) - (\mathbf{v} \cdot \nabla)\mathbf{B} \Rightarrow D_t \mathbf{B} = \mathbf{B} \cdot \nabla \mathbf{v} - \mathbf{B}(\nabla \cdot \mathbf{v})$$

Recall the density continuity equation: $D_t \rho = -\rho(\nabla \cdot \mathbf{v})$

The dynamical equation for $(\mathbf{B}/\rho)$ is obtained.

$$\boxed{\frac{D}{Dt}\left( \frac{\mathbf{B}}{\rho} \right) = \frac{1}{\rho}\frac{D\mathbf{B}}{Dt} - \frac{\mathbf{B}}{\rho^2}\frac{D\rho}{Dt} = \frac{\mathbf{B}}{\rho} \cdot \nabla \mathbf{v}}$$

Identical to the relation we have previously obtained for $d\mathbf{x}$ along the material line of the flow, which implies the following solution

$$\boxed{\frac{B_i\left( \mathbf{x}, t \right)}{\rho\left( \mathbf{x}, t \right)} = \frac{B_j\left( \mathbf{a}, 0 \right)}{\rho\left( \mathbf{a}, 0 \right)} \frac{\partial x_i}{\partial a_j}}$$

# Concepts: frozen-in magnetic field [3]

$$\frac{B_i(\mathbf{x},t)}{\rho(\mathbf{x},t)} = \frac{B_j(\mathbf{a},0)}{\rho(\mathbf{a},0)} \frac{\partial x_i}{\partial a_j}$$

**Note:** when the **Lorentze force is negligible**, $\partial x_i/\partial a_j$ and $B_i(\mathbf{x},t)$ are independent, this **is a solution** of the previous equation.

Let $d\mathbf{a}$ to be along the line of force at $t = 0$, so that $\mathbf{B}(\mathbf{a},0) \times \mathrm{d}\mathbf{a} = 0$, then at some later time $t$ we then have.

$$\left[\mathbf{B}(\mathbf{x},t)\times d\mathbf{x}(\mathbf{x},t)\right]_i = \varepsilon_{ijk} B_j(\mathbf{x},t) dx_k(\mathbf{a},t) = \varepsilon_{ijk} \frac{\rho(\mathbf{x},t)}{\rho(\mathbf{a},0)} B_m(\mathbf{a},0) \frac{\partial x_j}{\partial a_m} da_n \frac{\partial x_k}{\partial a_n}$$

Mass conservation: $\rho(\mathbf{x},t)\mathrm{d}^3\mathbf{x} = \rho(\mathbf{a},0)\mathrm{d}^3\mathbf{a}$, with Jacobian expression

$$d^3\mathbf{x} = J\, d^3\mathbf{a} \text{ and } J = \frac{\partial(x_1,x_2,x_3)}{\partial(a_1,a_2,a_3)} \text{ or } \varepsilon_{lmn}\, d^3\mathbf{x} = \varepsilon_{ijk} \frac{\partial x_i}{\partial a_l} \frac{\partial x_j}{\partial a_m} \frac{\partial x_k}{\partial a_n}$$

$$\varepsilon_{ijk} \frac{\rho(\mathbf{x},t)}{\rho(\mathbf{a},0)} B_m(\mathbf{x},t) \frac{\partial x_j}{\partial a_m} da_n \frac{\partial x_k}{\partial a_n} = \varepsilon_{lmn} \frac{\partial a_l}{\partial x_i} B_m(\mathbf{a},0) da_n$$

$$\boxed{\left[\mathbf{B}(\mathbf{x},t)\times d\mathbf{x}(\mathbf{a},t)\right]_i = \left[\mathbf{B}(\mathbf{a},0)\times d\mathbf{a}\right]_l \frac{\partial a_l}{\partial x_i} = 0}$$

# Magnetic field line topology [2, 4]

Magnetic field lines are material lines of $\mathbf{B}\rho^{-1}$ advected by the flow $\mathbf{v}$.

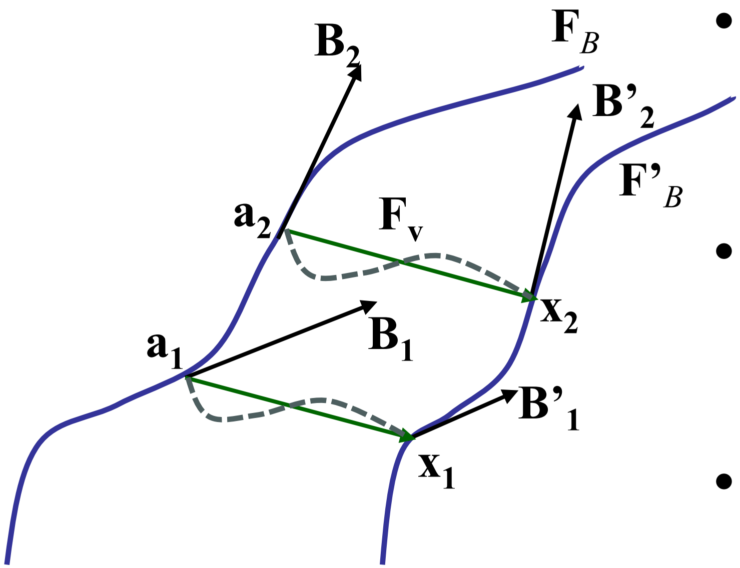


- At $t = 0$, points $\mathbf{a}_1$, $\mathbf{a}_2$ lie on the same magnetic field line $\mathbf{F}_\mathrm{B}$ parametrised by $p$
- A plasma parcel at $\mathbf{a}_{1(2)}$ moves to $\mathbf{x}_{1(2)}$ along the material line $\mathbf{F}_\mathrm{v}$ parametrised by time $t$
- Points $\mathbf{x}_1$, $\mathbf{x}_2$ lie on the same field line $\mathrm{F'}_\mathrm{B}$

Magnetic topology is conserved if a velocity vector field $\mathbf{v}(\mathbf{x},t)$ and a scalar function $\alpha(\mathbf{x},t)$ exist, so that [2]:

$$\boxed{\partial_t \mathbf{B} + \mathbf{v}\cdot\nabla\mathbf{B} - \mathbf{B}\cdot\nabla\mathbf{v} = \alpha\mathbf{B}}$$

- **Allows local changes of topology at magnetic null points**
- Stronger than ‘field line conservation’: $(\mathbf{B}\cdot\nabla\mathbf{v} - \alpha\mathbf{B})\times\mathbf{B} = 0$


**[2]** Hornig & Schindler, Physics of Plasmas 3, 781 (1996); **[4]** Lau & Finn, Astrophys. J., 350:672-691 (1990);

# Magnetic helicity

A measure of magnetic field complexity in a volume is magnetic helicity

$$\boxed{I = \int_V \mathbf{A}\cdot\mathbf{B}\, d^3\mathbf{x}}$$

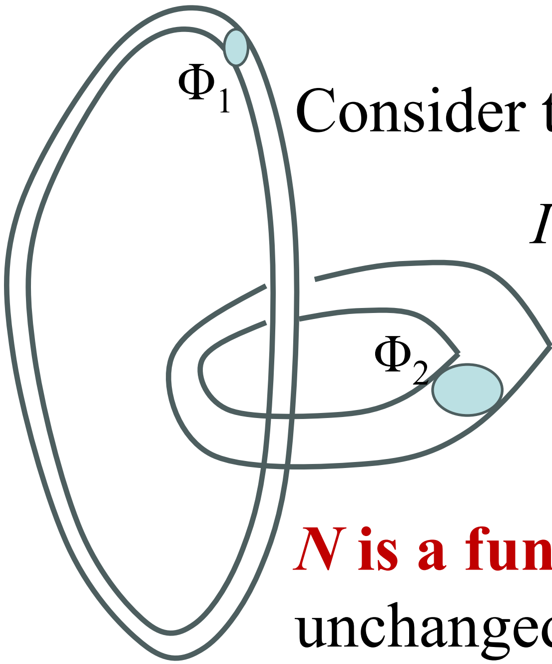


Consider two flux tubes linked together, as shown to the left.

$$I_1 = \int_{C1} \mathbf{A}\cdot d\mathbf{l} \iint_{S1} \mathbf{B}\cdot\mathbf{n}\, dS = \Phi_1 \oint_{C1} \mathbf{A}\cdot d\mathbf{l} = \Phi_1\Phi_2$$

*N-times* linked flux tubes: $I = \pm N\Phi_1\Phi_2$

A single knotted flux tube with *m* knots: $I = \Phi^{\mathrm{m}}$

***N* is a fundamental topological invariant**, as it remains unchanged under continuous deformations of the flux tubes.

- $I$ must be integrated over the entire space, and $\mathbf{A}\rightarrow 0$ as $\mathbf{x} \rightarrow \pm\infty$
- If the volume is finite, we **must** have boundaries at which $\mathbf{B}\cdot\underline{\mathbf{n}}|_{\mathrm{S}} = 0$.

If these criteria are not met the magnetic field line can leave the volume and cannot be accounted for in the integral.

# Magnetic helicity conservation

If the magnetic field lines are frozen into plasma flow, their global topological structure cannot change with time.

$$\frac{D}{Dt}\left(\frac{\mathbf{A}\cdot\mathbf{B}}{\rho}\right)=\mathbf{A}\cdot\frac{D}{Dt}\left(\frac{\mathbf{B}}{\rho}\right)+\frac{\mathbf{B}}{\rho}\cdot\frac{D\mathbf{A}}{Dt}=\frac{\mathbf{B}}{\rho}\cdot\nabla\mathbf{v}+\frac{\mathbf{B}}{\rho}\cdot\left(\frac{\partial\mathbf{A}}{\partial t}+\mathbf{v}\cdot\nabla\mathbf{A}\right)$$

For the ideal MHD $\mathbf{E} = -\mathbf{v}\times\mathbf{B}$ and the Maxwell equations give

$\mathbf{E}=\dfrac{\partial\mathbf{A}}{\partial t}-\nabla\phi$ and vector identity $\mathbf{v}\times(\nabla\times\mathbf{A})=\mathbf{v}\times\mathbf{B}=\nabla\mathbf{v}\cdot\mathbf{A}-\mathbf{v}\cdot\nabla\mathbf{A}$

$$\frac{D}{Dt}\left(\frac{\mathbf{A}\cdot\mathbf{B}}{\rho}\right)=\left(\frac{\mathbf{B}}{\rho}\cdot\nabla\right)\left(\mathbf{A}\cdot\mathbf{v}-\phi\right)$$

Consider a flux tube frozen into the field so that $\mathbf{n}\cdot\mathbf{B}|_S = 0$ permanently

$$\boxed{\frac{dI}{dt}=\int_V\frac{D}{Dt}\left(\frac{\mathbf{A}\cdot\mathbf{B}}{\rho}\right)\rho\, d^3\mathbf{x}=\int_V\left(\mathbf{B}\cdot\nabla\right)(\mathbf{A}\cdot\mathbf{v}-\phi)d^3\mathbf{x}=\int_S(\mathbf{n}\cdot\mathbf{B})(\mathbf{A}\cdot\mathbf{v}-\phi)dS=0}$$

# Magnetic topology near a null

Since local magnetic field line topology of the perfectly conducting plasma is conserved everywhere but at magnetic null points, if we characterise the local topology near the null, we know that it will be preserved when advected.

There are **two distinct magnetic field line configurations** that can support a null point: **parabolic field lines or o-points** and **hyperbolic field lines or x-points** [4].

**Parabolic lines (o-point) and Hyperbolic lines (x-point) [5]**

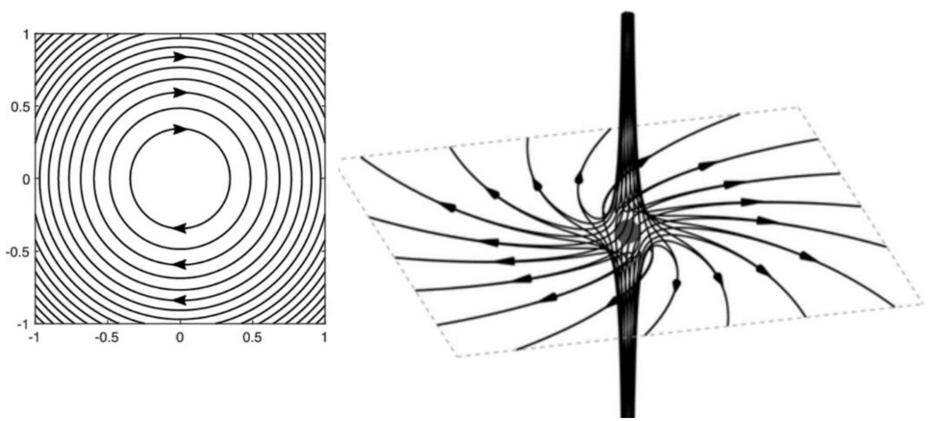

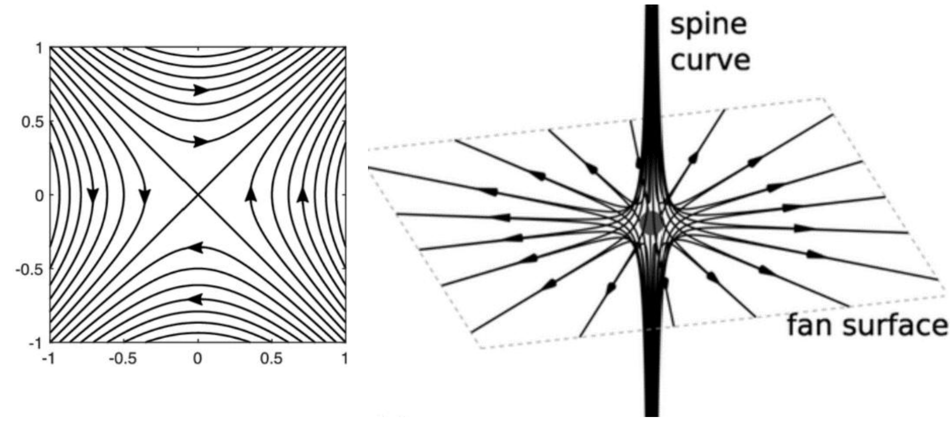


**[4]** Lau & Finn, Astrophys. J., 350:672-691 (1990); **[5]** Pontin & Priest, *Living Rev. Solar Phys*. 19 (2022)

# Local magnetic topology

Consider a set of magnetic field lines in a finite volume $V$ of the ideal plasma. The magnetic field line topology near a null point can be deduced from the simultaneous measurements of magnetic field at a set of arbitrary points.

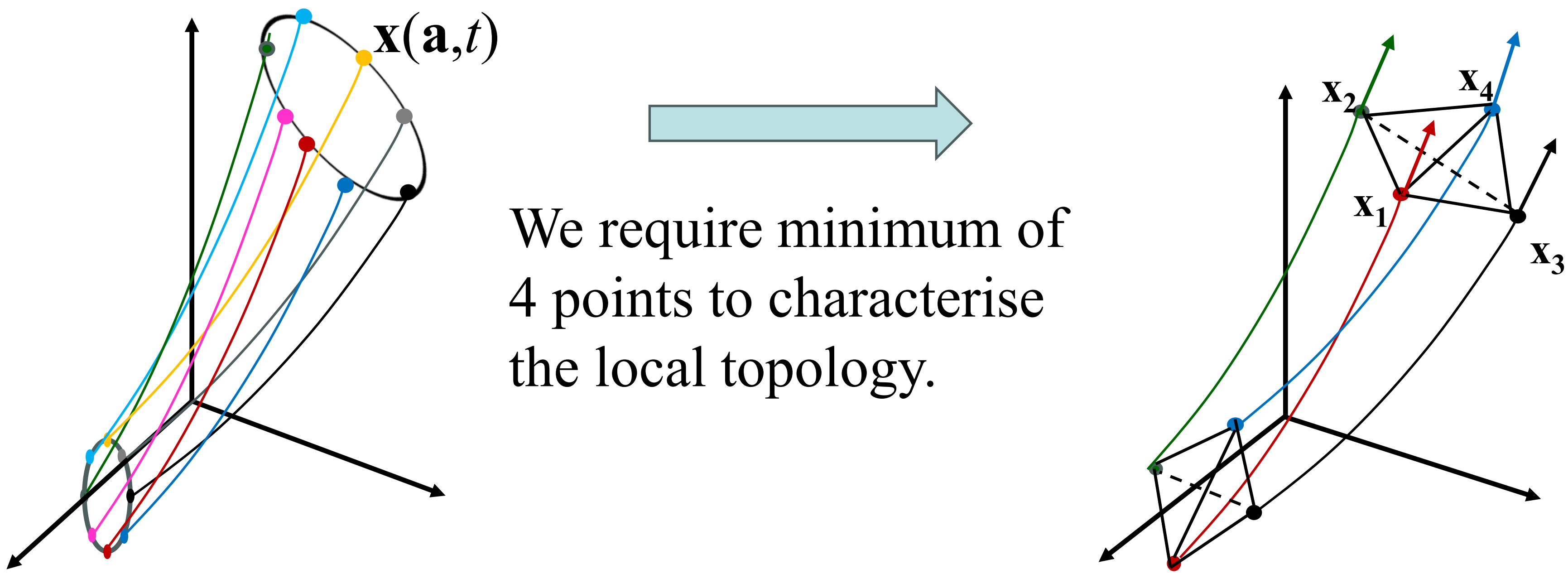


We require minimum of 4 points to characterise the local topology.

Let us place the null at the centre of mass $\mathbf{x}_c$. Taylor expansion gives

$$\mathbf{B}(\mathbf{x}_i) = \mathbf{B}(\mathbf{x}_c) + \nabla\mathbf{B}\cdot(\mathbf{x}_i - \mathbf{x}_c) + \ldots = \nabla\mathbf{B}\cdot\boldsymbol{\rho}$$

# Magnetic field gradient tensor

All topological information about the field configuration near a null point is contained in the magnetic field gradient tensor **A**

$$\boxed{M_{ij} = (\nabla \mathbf{B})_{ij} = \frac{\partial B_i}{\partial r_j}}$$

Let us assume that we can construct a true gradient of the magnetic field vector at a point. **How do we extract topological information**?

The topology characterisation is reduced to an eigenvalue problem for $M_{ij}$. The characteristic equation det($\mathbf{M}$-$\lambda\mathbf{I}$) = 0 is expressed as

$$|\mathbf{M} - \lambda_i \mathbf{I}| = \lambda_i^3 + P\lambda_i^2 + Q\lambda_i + R = 0$$

where the coefficients are the topological invariants $P$, $Q$ and $R$

$$\boxed{\begin{aligned} P &= -\mathrm{Tr}(\mathbf{M}) = -(\lambda_1 + \lambda_2 + \lambda_3) = 0 \\ 2Q &= P^2 - \mathrm{Tr}(\mathbf{M}^2) = \lambda_1\lambda_2 + \lambda_1\lambda_3 + \lambda_2\lambda_3 \\ 3R &= -P^3 + 3PQ - \mathrm{Tr}(\mathbf{M}^3) = -\lambda_1\lambda_2\lambda_3 \end{aligned}}$$

# Magnetic field gradient tensor

We can transform to canonical basis, in which **M'** is diagonal.

$$\text{Case 1: } \mathbf{M}' = \begin{bmatrix} \sigma & -\omega & 0 \\ \omega & \sigma & 0 \\ 0 & 0 & b \end{bmatrix} \text{ if } \lambda_{1,2} = \sigma \pm i\omega \in \mathbb{C}, b \in \mathbb{R}$$

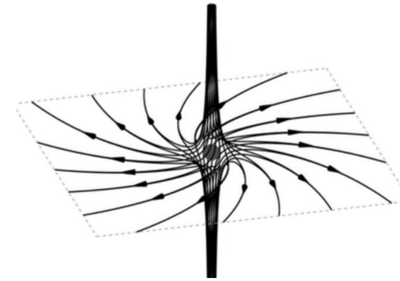

$$\text{Case 2: } \mathbf{M}' = \begin{bmatrix} \lambda_1 & 0 & 0 \\ 0 & \lambda_2 & 0 \\ 0 & 0 & \lambda_3 \end{bmatrix} \text{ if } \lambda_i \in \mathbb{R}$$

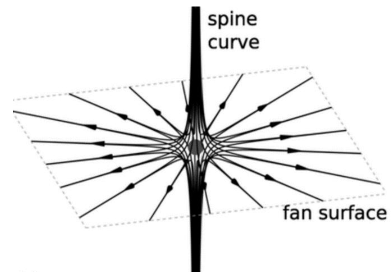


$$\boldsymbol{D = (27/4)\, R^2 + Q^3 = 0}$$

Curve $D(R,Q)$ divides the $(R,Q)$ plane into 2 regions:

**Hyperbolic lines: $D < 0$**

**Elliptic lines : $D > 0$**

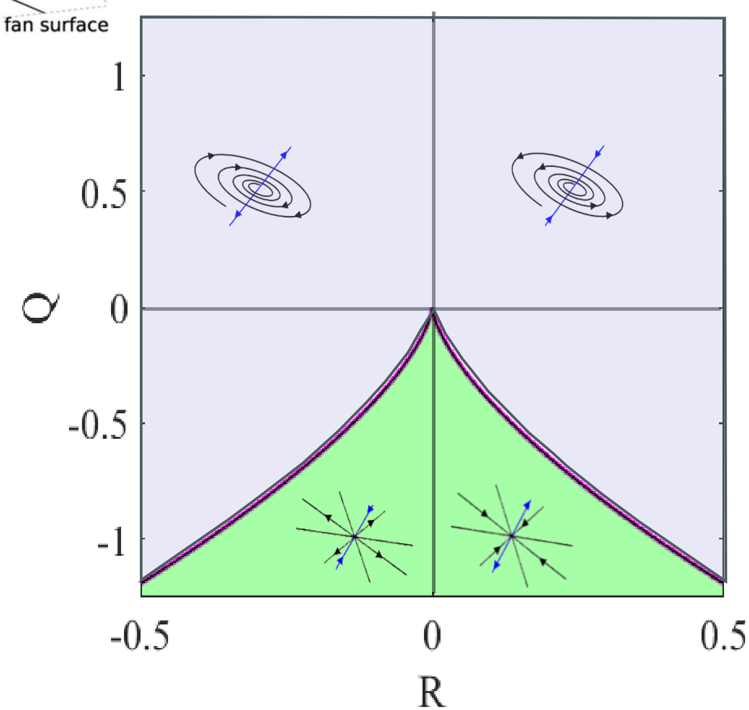

# Evolution of local magnetic topology [6]

Given a single Eulerian measure of the topological invariants, we can also access their evolution. First, the MHD equations are written using gradient tensors of the velocity **A** and of the magnetic field **M:**

$$\dot{\mathbf{A}} = -\mathbf{A}^2 + \frac{\eta}{\rho}\nabla^2\mathbf{A} + \frac{1}{3}\left[-\frac{1}{2\rho}\mathrm{Tr}(\mathbf{\Xi}^2) + \mathrm{Tr}(\mathbf{A}^2)\right]\mathbf{I} + \frac{1}{\rho}\left(\mathbf{\Xi}\cdot\mathbf{M} + \mathbf{B}\cdot\nabla\mathbf{M}\right)$$

$$\dot{\mathbf{M}} = [\mathbf{A},\mathbf{M}] + \mathbf{B}\cdot\nabla\mathbf{M} + \chi\nabla^2\mathbf{M},$$

where $\mathbf{\Xi} = \mathbf{M} - \mathbf{M}_{\mathrm{T}}$, is twice the antisymmetric part of the magnetic field gradient tensor, related to current density, $\Xi_{ik} = \varepsilon_{ikl}\, j_l$.

Then by using the definitions of invariants their Lagrangian time evolution can be derived and visualised in the $(R,Q)$ plane.

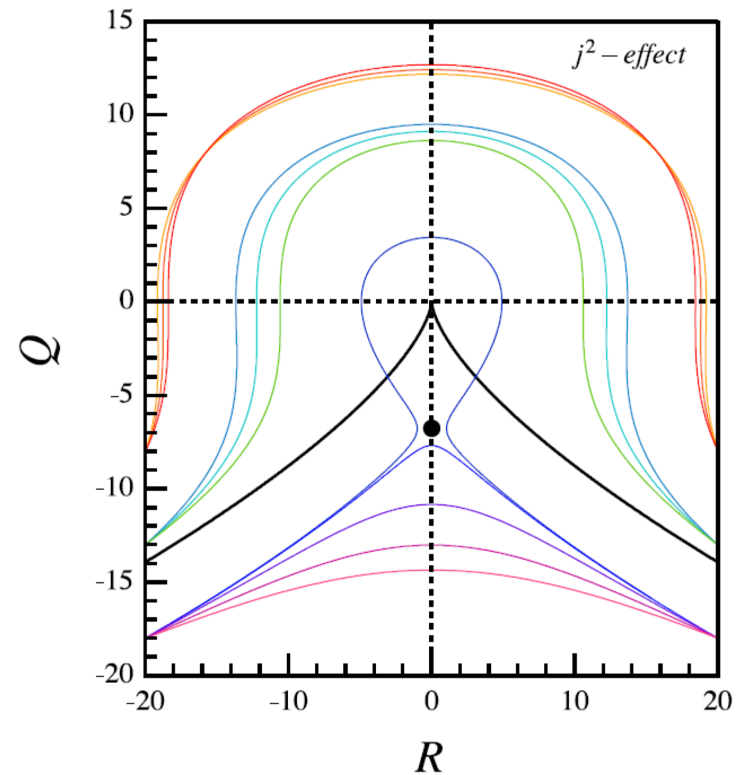


**[6]** Quattrociocchi et al., *The Astrophysical Journal*, **878** (2019).

# Part II: Application of magnetic field line topology in space plasmas

- Why is magnetic topology of interest
- Magnetic field gradient tensor reconstruction from 4 spacecraft
- Sources of uncertainties
- Examination of single null magnetosheath reconnection event
- Topological invariants in the studies of turbulence

# Why is it important?

- Fundamental processes in space plasma, such as turbulence and magnetic reconnection are associated with magnetic field structures and magnetic field configurations.

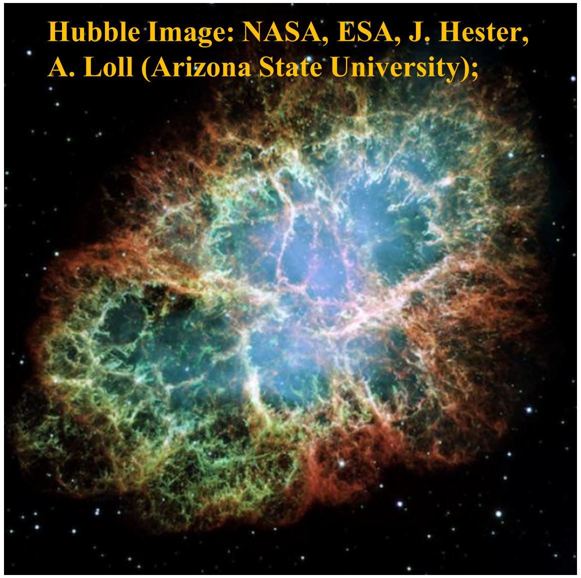


- **Turbulence:** efficient dissipation needs small scale structures such as stretched turbulent vortices or thin reconnecting current sheets [7, 8].

- **3D Reconnection:** initial local x-point-like configuration may evolve multiple finite length flux ropes with x-point like magnetic field configurations in between them [9].

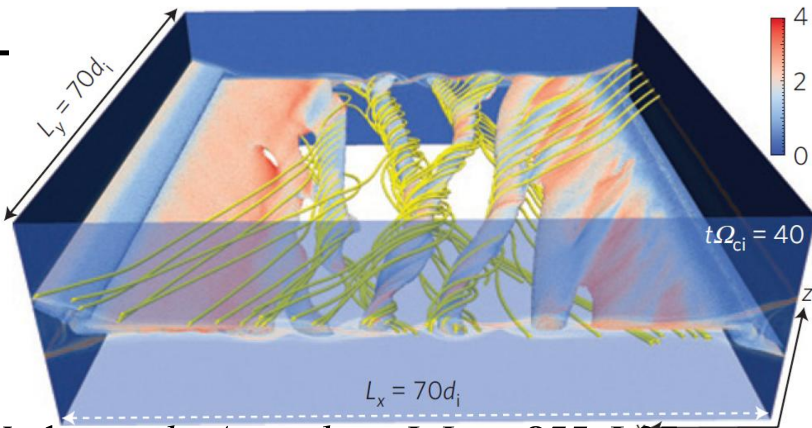


**[7]** Boldyrev and Loureiro, *Astrophys. J.* **844**, 125 (2017); **[8]** Vech, *et. al.*, *Astrophys. J. Lett.* **855**, L27 (2018); **[9]** Daughton *et al.*, *Nature Phys.*, **7** 539 (2011)

# Magnetic field gradient tensor [10]

## How do we construct an estimate of M from 4 spacecraft formation?

Spacecraft $a = 1,\ldots,4$ measure magnetic field vector $\mathbf{B}^a$ at position $\mathbf{x}^a$.
It in the centre of mass frame

$$\mathbf{x}^c = \sum_{a=1}^{4} \mathbf{x}^a \text{ and } \mathbf{B}^c = \sum_{a=1}^{4} \mathbf{B}^a$$

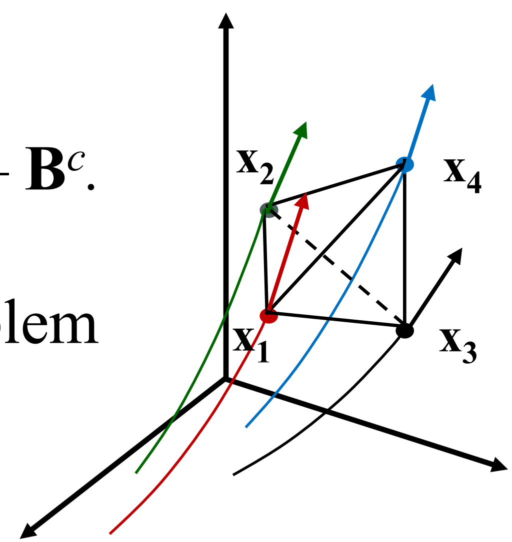


In this frame of reference: $\mathbf{r}^a = \mathbf{x}^a - \mathbf{x}^c$ and $\mathbf{b}^a = \mathbf{B}^a - \mathbf{B}^c$.

The estimate of the gradient is an optimisation problem

$$\boxed{S = \sum_{i=1}^{3} \sum_{a=1}^{4} \left( b_i^a - \sum_{j=1}^{3} r_j^q M_{ji} \right)^2 + \zeta \sum_{i=1}^{3} M_{ii}}$$

The last term is the Lagrange multiplier that represents $\nabla \bullet \mathbf{B} = 0$
The condition for minimal S, found from dS/dM = 0, is

$$\sum_{k=1}^{3} g_{ik} M_{kj} + \zeta \delta_{ij} = W_{ij} \text{ where } g_{ij} = \sum_{a=1}^{4} r_i^a r_j^a \text{ and } W_{ij} = \sum_{a=1}^{4} r_i^a b_j^a$$

**[10]** A. Pumir *et al.*, Physics of Fluids 25, 035101 (2013);

# Magnetic field gradient tensor

Including the constrain condition, the method gives the optimal solution

$$\boxed{\mathbf{M} = \mathbf{g}^{-1}\mathbf{W} - \frac{1}{3}\mathrm{Tr}(\mathbf{g}^{-1}\mathbf{W})}$$

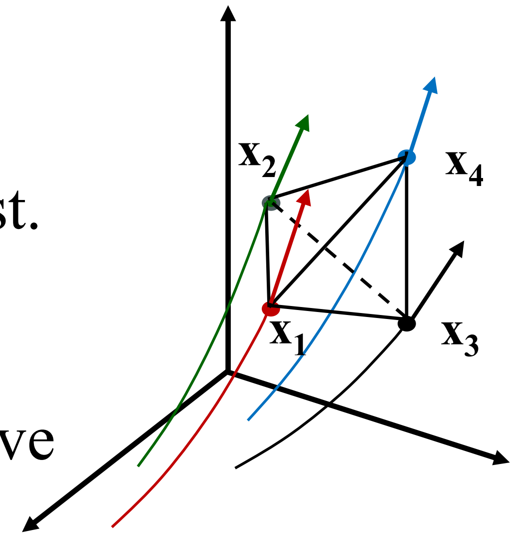


- Matrix **g** must be invertible for the solution to exist.
- This a symmetric matrix and hence can be diagonalised. All eigenvalues $\gamma_i$ are real and positive
- $L_i = (\gamma_i)^{1/2}$ is a characteristic length of the tetrahedron in the direction of the *i*-th eigenvector.
- For inverse to exist we must have all $\gamma_i \neq 0$, thus the **spacecraft configuration cannot be co-planar**.

This estimate is called **volume-averaged** or **coarse-grained** magnetic field gradient tensor

$$\boxed{M_{ij} \equiv \frac{1}{V}\int_V \frac{\partial B_i}{\partial r_j} d^3r}$$

# Tensor construction

- Number of spatial points allows only the linear approximation in the Taylor expansion.
- Only **constant gradient on the scale of the tetrahedron or larger** is measured.

$$\boxed{B_i^{sc} = B_{i,0} + \frac{\partial B_i^{sc}}{\partial x}\left(x - x_0\right) + \frac{\partial B_i^{sc}}{\partial y}\left(y - y_0\right) + \frac{\partial B_i^{sc}}{\partial z}\left(z - z_0\right)}$$

- 12 unknowns: 4 unknowns in each equation; $i$ = x, y, z, and $sc$ = 1,..,4
- 12 equations: 3 components of **B** measured at 4 points

This is **a well-posed problem** which can be solved by, for example, the least square method polynomial fit.

Note that this approach allows for the solenoidal constrain to be added to this solution quite naturally.

# Beyond linear approximation [11]

Suppose we Taylor-expand **B** around each spacecraft to second order in separations

$$B_i^{sc} = B_{i,0} + \frac{\partial B_i^{sc}}{\partial x}\Delta x + \frac{\partial B_i^{sc}}{\partial y}\Delta y + \frac{\partial B_i^{sc}}{\partial z}\Delta z + \frac{1}{2}\frac{\partial^2 B_i^{sc}}{\partial x^2}(\Delta x)^2 + \frac{1}{2}\frac{\partial^2 B_i^{sc}}{\partial y^2}(\Delta y)^2 + \frac{1}{2}\frac{\partial^2 B_i^{sc}}{\partial z^2}(\Delta z)^2 +$$

$$\frac{\partial^2 B_i^{sc}}{\partial x \partial y}\Delta x\Delta y + \frac{\partial^2 B_i^{sc}}{\partial x \partial z}\Delta x\Delta z + \frac{\partial^2 B_i^{sc}}{\partial y \partial z}\Delta y\Delta z$$

10×3 = **30 unknowns, 12 equations** – the problem is not well defined

Modern spacecraft measure **particle currents** to a reasonable accuracy and on reasonable time scales. Use the **current measurements** to further **restrict the field** using: $\nabla \times \mathbf{B}^{sc} = \mu_0 \mathbf{j}^{sc}$

12 equations from Taylor expansion of **B**

12 equations from current measurements

4 equations from $\nabla \bullet \mathbf{B} = 0$

**Total number of equations**: 12 + 12 + 4 = 28. Need more restrictions…

**[11]** R. E. Denton, et al., JGR 127 (2022)

# Local LMN coordinate system

If the magnetic configuration is anisotropic, we can identify the direction of the minimum variation of the magnetic field.

For example, in approximately 2D reconnecting current sheet M is the direction of minimum variance of magnetic field.

We can then neglect all second order terms with second derivatives in M direction in Taylor expansion.

This leaves us with **27 unknowns and 28 equations**. The problem is now well defined.

The derivatives can be found using the nonlinear least square fits for 24 equations and divergence-free condition is used as a constraint.

# Gradient tensor elements error [12]

The **most significant error is due to the tetrahedron geometry**, given by elongation and planarity parameters. Let $a^2 > b^2 > c^2$ be the eigenvalues of matrix **g**.

**Elongation**: $E = 1 - (b/a)$ **Planarity**: $P = 1 - (c/b)$

Reliable estimate of the magnetic field gradient tensor requires these parameters to be below certain values, say $E, P < 0.3$.

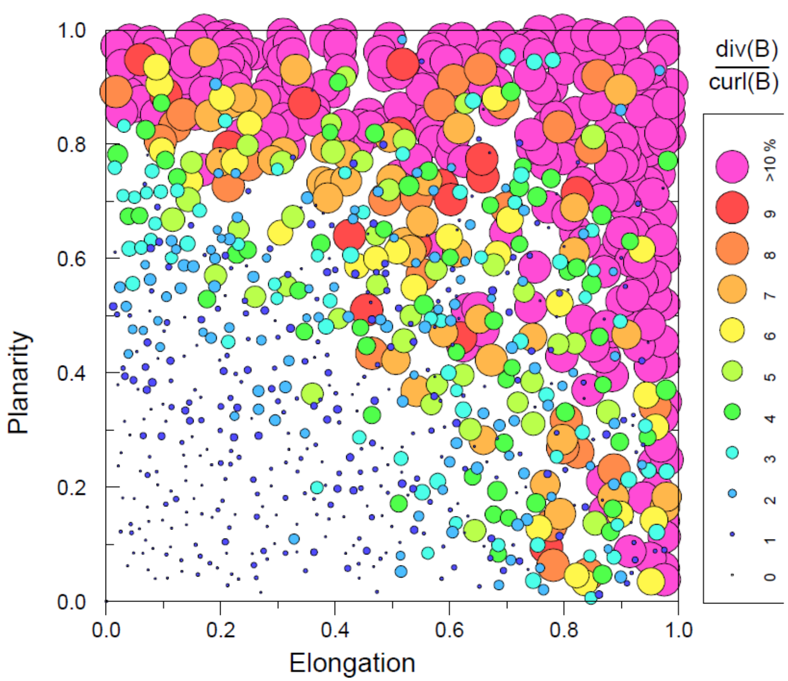


Uncertainty in current estimate, the anti-symmetric part of the gradient tensor:

$$er_j \sim \frac{\nabla \cdot \mathbf{B}}{\left|\nabla \times \mathbf{B}\right|}$$

Other sources of error:
Magntometer error ~ 0.1 nT, spacecraft position, timing

[12] G. Paschmann and P.W. Daly, Analysis methods for multi-spacecraft data, Scientific Reports (1998)

# Four-spacecraft missions [13-16]

- Minimum 4 no co-planer points needed to construct **M**.
- Cluster and MMS missions satisfy this requirement

| | **Cluster mission** | **Magnetospheric Multi-Scale (MMS)** |
|---|---|---|
| $L_i$ in the solar wind | 30-200 $\rho_p$ | ~1 $\rho_p$ |
| FGM sampling | 22 Hz | 1024 Hz |
| SCM sampling | 410 Hz | 8192 Hz |
| Ion sampling | 0.25 Hz | 1 Hz |
| Electron sampling | 0.25 Hz | 33 Hz |

- Cluster's characteristic size of formation in the solar wind: ~100 $\rho_p$, near the limit of applicability of the MHD
- MMS characteristic size of formation in the magnetosheath: ~1 $\rho_p$ is below the MHD scale

[13] A. Balogh *et al*., Space Sci. Rev. 79, 65 (1997); [14] H. Réme *et al*., Ann. Geophys. 19, 1303 (2001);
[15] Russell, C. T. *et al*., Space Sci. Rev. 199 (2016); [16] Lindgvist P.A. *et al*., Space Sci. Rev. 199 (2016).

# Magnetic reconnection

**Magnetic reconnection:** transient conversion of magnetic energy to plasma, particles and waves associated with the change in the magnetic field line topology.

MHD description with resistive Ohm's law ($\mathbf{E} = -\mathbf{v} \times \mathbf{B} + \mathbf{j}/\sigma$) gives slow reconnection rates and describes the physics on scales $l > \rho_\mathrm{i} > d_\mathrm{i}$

- Astrophysical plasmas are collisionless, resistivity is not a dominant feature
- Two fluid description (electron and ion fluid) generalises Ohm's law, and in its simplest form only the Hall term is retained [17]

$$\mathbf{E} + \mathbf{v}_i \times \mathbf{B} - \frac{\mathbf{j} \times \mathbf{B}}{n_e e} = \frac{\mathbf{j}}{\sigma} \quad \text{and} \quad \mathbf{j} = e n_e (\mathbf{v}_i - \mathbf{v}_e)$$

**Hall term becomes important when length scale $d_\mathrm{i} \sim c/\omega_{\mathrm{pi}} = v_A/\omega_{\mathrm{ci}}$**

[17] Treumann & Baumjohann Frontiers in Physics 2013;

# Magnetic reconnection

Figure 4 of [18]

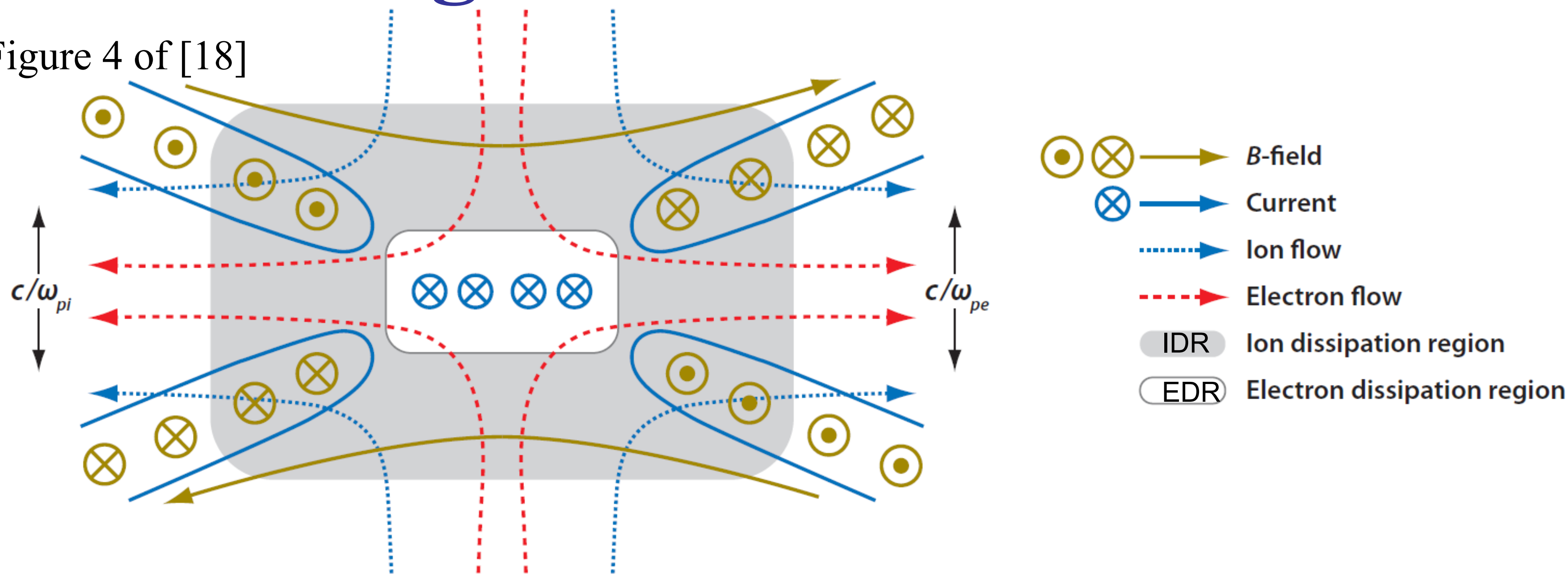


- Current sheet length comparable to electron mean free path
- Ions are demagnetised, ion inertial effects dominate in IDR
- Electrons remain magnetised, their **E**×**B** drift supports Hall current, which peaks at the EDR where the X-point (magnetic null) resides
- At the scale of $d_i$, magnetic field is advected by electron fluid and the topology is conserved

[18] Zweibel & Yamada, Annu. Rev. Astron. Astrophys. 2009.

# Solar wind / magnetosheath plasma

- **Solar wind**: stream of supersonic and super-Alfvénic electrons, protons (96%), ions (4%)
- $V_{sw} \sim 500$ km/s, $n_{sw} \sim 5$ cm$^{-3}$, $|B| \sim 5$ nT, $\beta \sim 1$
- Includes solar flares, coronal mass ejections
- "Natural laboratory" for **MHD turbulence**

- **Magnetosheath:** interface between solar wind and the magnetosphere. Solar wind slows down, undergoes heating and is diverted around the magnetosphere.
- For southern IMF reconnection may occur
- $V_{MS} \sim 200$ km/s, $n_{MS} \sim 25$ cm$^{-3}$, $|B| \sim 50$ nT, $\beta \sim 1$

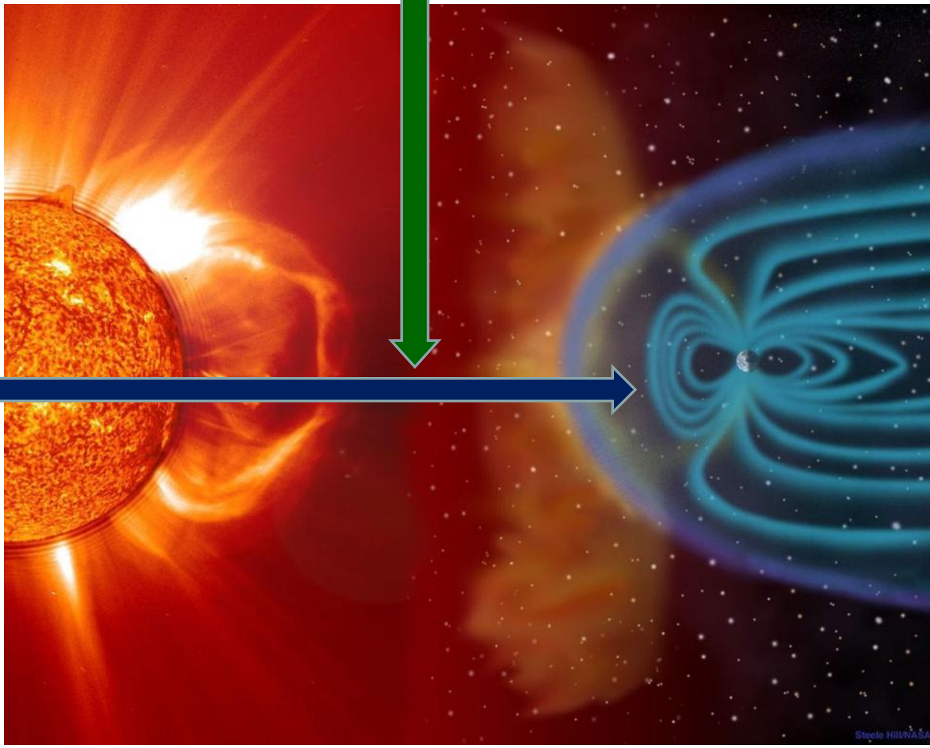

# Magnetic topology and reconnection

**Question: how does magnetic topology near the electron diffusion region (EDR) effect electron energisation process.**

Magnetopause reconnection event from MMS 19-Sep-2015 [19,20]

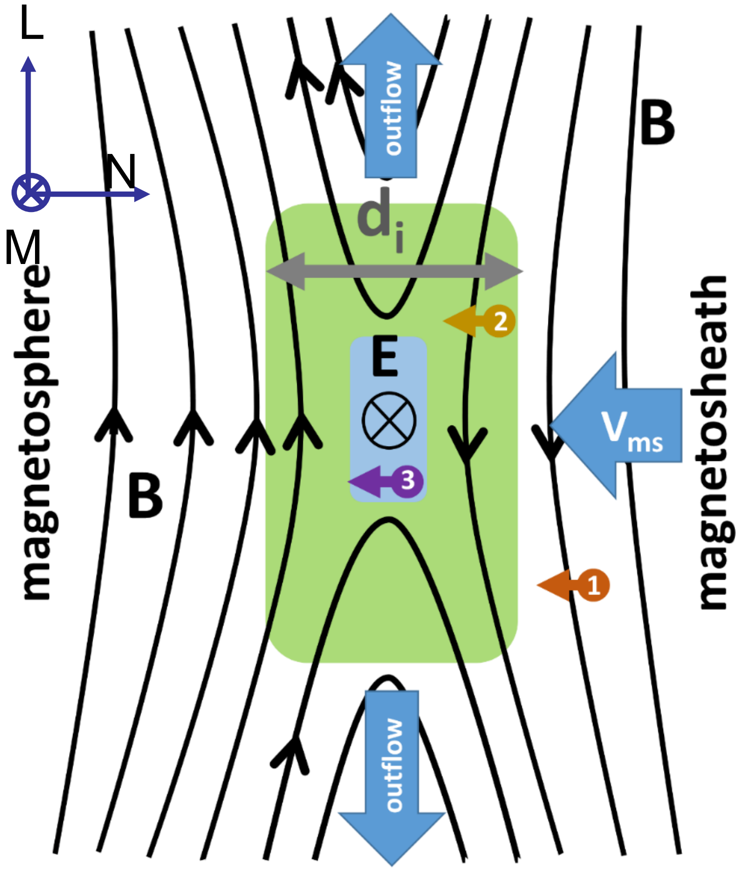


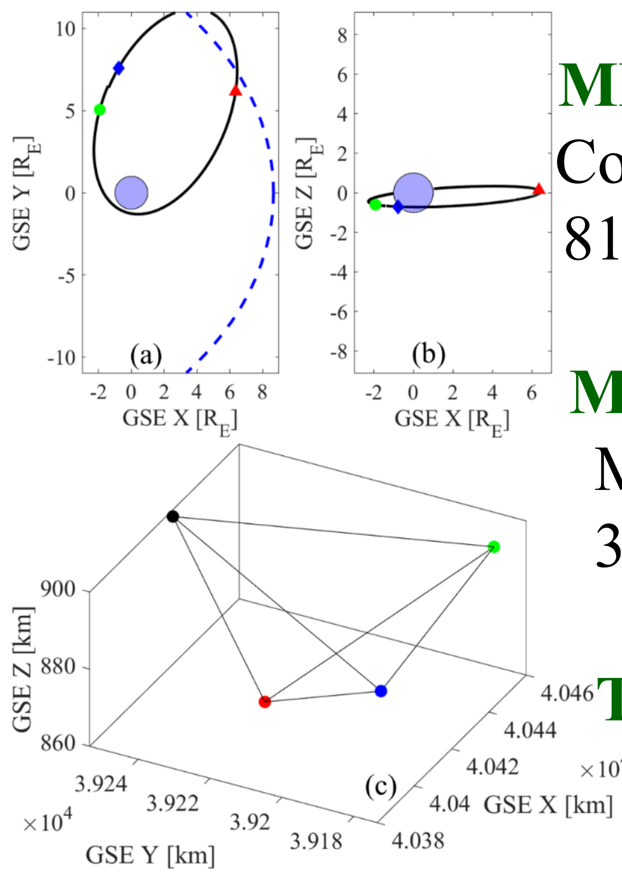


**MMS Magnetic data:**
Combined FGM+SCM
8192 samples / second

**MMS Electron data:**
Moments FPI-DEM
33 samples / second

**Tetrahedron scale:**
~70 km or 1 $\rho_p$


**[19]** Chen, L. J. *et al., Geophys. Res. Lett.* **43**, (2016); **[20]** Hnat, B., *et al*., (2023), *Scientific Reports*,

# Magnetic field line topology

Let $\lambda_1$, $\lambda_2$, $\lambda_3$ be the eigenvalues of **M**. Tensor invariants $Q$, $R$ are:

$$2Q = -\mathrm{Tr}(\mathbf{M}^2) = \lambda_1\lambda_2 + \lambda_1\lambda_3 + \lambda_2\lambda_3 \quad 3R = -\mathrm{Tr}(\mathbf{M}^3) = -\lambda_1\lambda_2\lambda_3$$

Magnetic field line topology classification [7]: $\boldsymbol{D = (27/4)\, R^2 + Q^3}$

- **Elliptic lines** (flux tubes & plasmoids): $D > 0$, $\lambda_1$, $\lambda_2$ in $\mathbb{C}$, $\lambda_3$ in $\mathbb{R}$
- **Hyperbolic field lines** (X-point): $D < 0$, $\lambda_1$, $\lambda_2$, $\lambda_3$ in $\mathbb{R}$

$$M_{ij} = S_{ij} - \frac{1}{2}\varepsilon_{ijk} J_{ij}$$

- $S_{ij}$: curl-free deformations of magnetic field lines
- Invariants $R_s$, $Q_s$
- $D_s = (27/4)\, R_s^2 + Q_s^3$

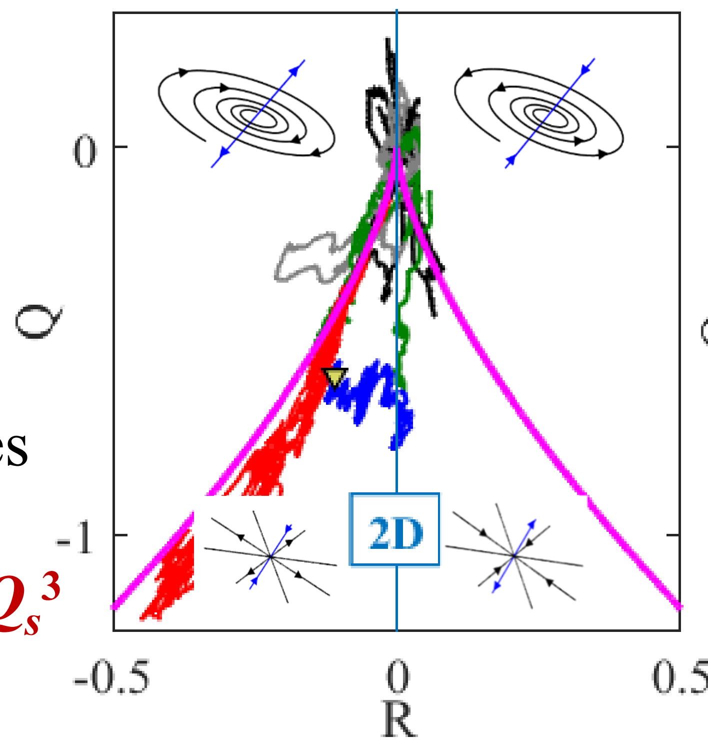


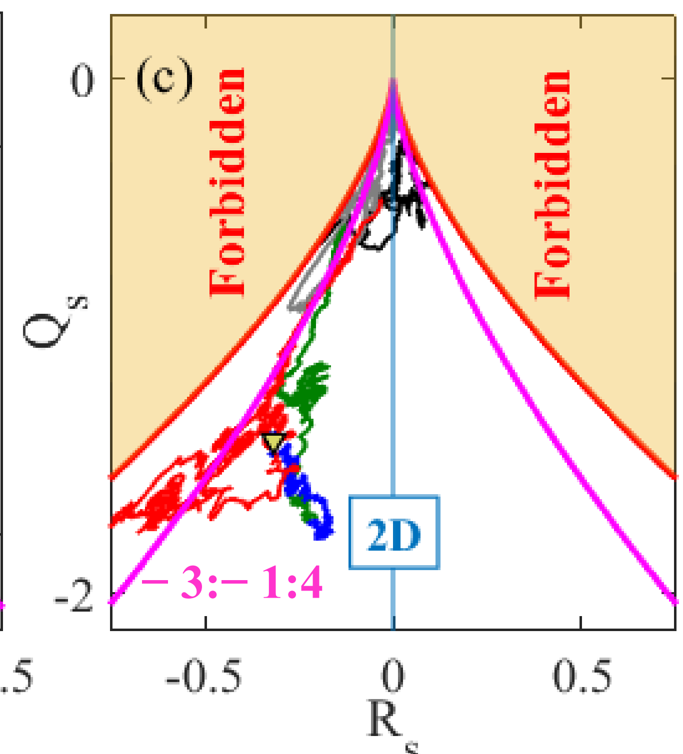

# Magnetic topology near null point

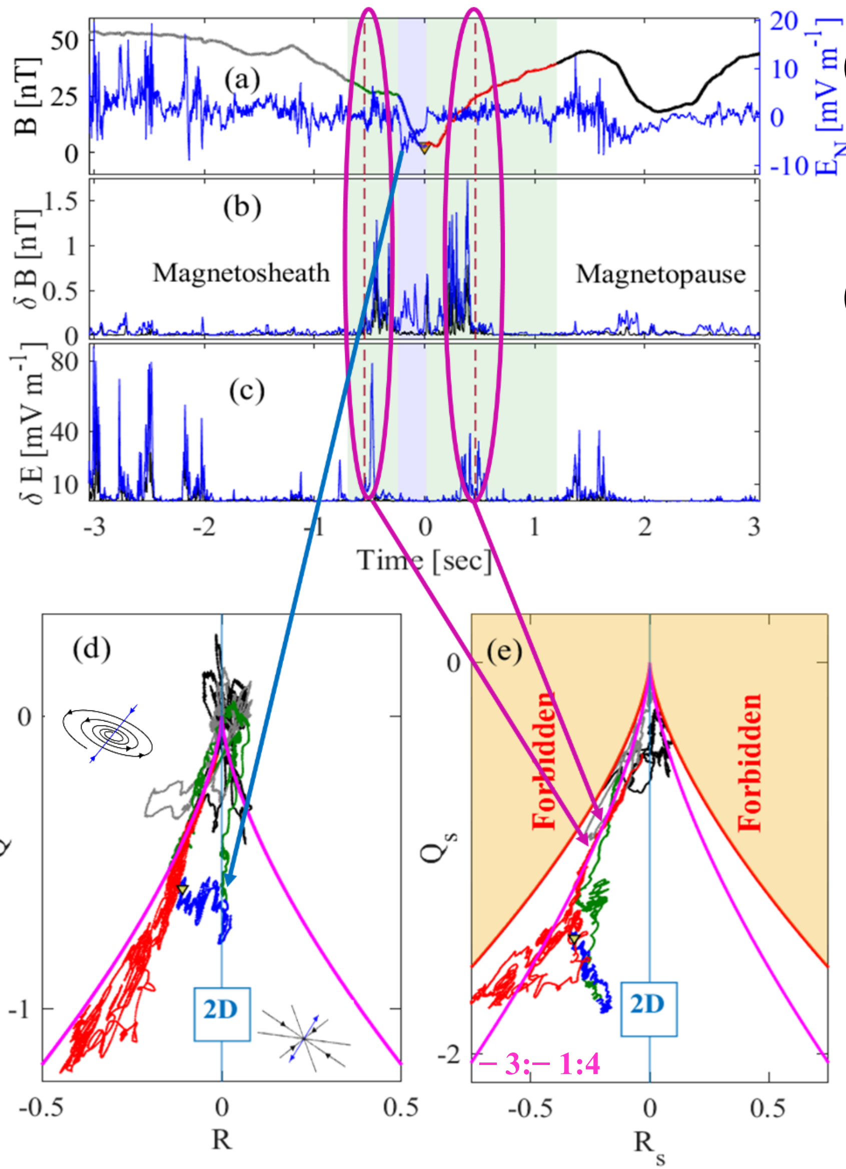


(a) **EDR:** Large increase in electric field across the current sheet, magnetic null

(b) Large magnetic and electric fields fluctuations at the **edges of the EDR**

**(d) Invariants *R*, *Q*:** The **EDR** has **reduced dimensionality**, appear to be nearly 2D.

**(e) Invariants $R_s$, $Q_s$**, curl-free deformations of B field. **Turbulent-type topology** of biaxial contraction of magnetic structures.

# Electron physics and magnetic topology

**Suprathermal electron beam, $\mathcal{E}_e$:**

- Integrated differential electron flux in energy range 800-$10^4$ eV
- Accelerated at the EDR (near X-point) where magnetic field line topology tends to 2D

**Bulk electron temperature anisotropy, $\alpha_e$**

- Increases near the edge of the EDR where magnetic field topology has turbulence-like features
- Magnetic structures evolve in a similar way to the 3D HD collapsing vortices (same eigenvalue ratio)

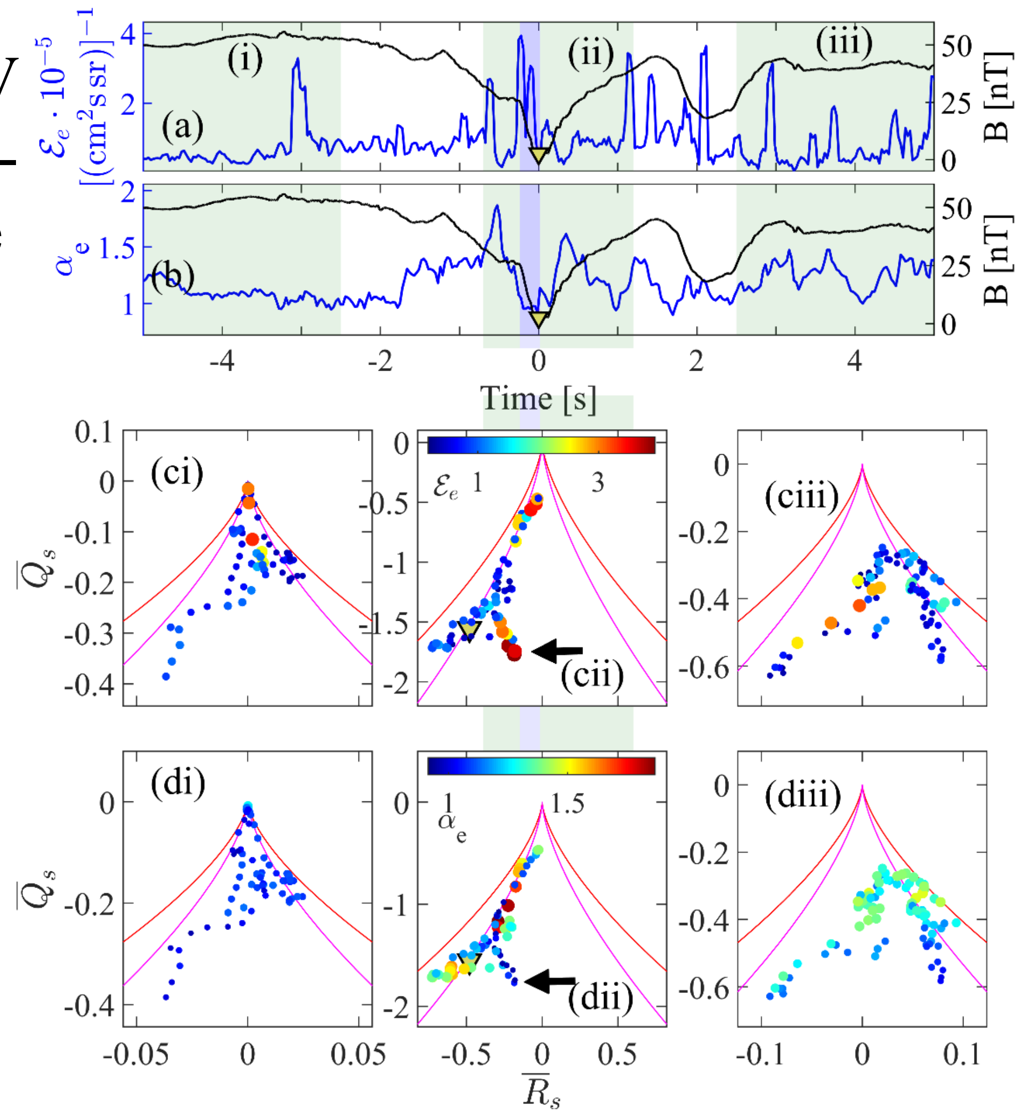

# Magnetic structures and turbulent heating of solar wind

- Solar wind **expands into the heliosphere non-adiabatically**
- Injected solar energy is converted to heat via wave-particle **resonances, turbulence and reconnection**.
- Solar wind observations show features consistent with nonlinear energy transfer from large to small spatial scales. We refer to such energy transfer as **turbulent energy cascade**.
- Turbulence and reconnection generate magnetic structures: flux tubes, current sheets, X- and O-points. Simulations and observations suggest that these are preferential heating sites.

**Question: is turbulent energy transfer rate the same in all magnetic structures?**

# Statistical approach to turbulence

Yaglom's law relates third order product of fluctuations, defined as, $\delta\mathbf{a} = \mathbf{a}(\mathbf{x}+\mathbf{r}) - \mathbf{a}(\mathbf{x})$ and the **average** turbulent cascade rate $\varepsilon$

$$S_r = Y_r + \frac{1}{2}H_r = -\frac{4}{3}\varepsilon r$$

$$Y_r = \left\langle \delta \mathrm{v}_r \left( |\delta\mathbf{v}|^2 + |\delta\mathbf{b}|^2 \right) - 2\delta b_r (\delta\mathbf{v}\cdot\delta\mathbf{b}) \right\rangle; \quad H_r = \left\langle \delta b_r (\delta\mathbf{j}\cdot\delta\mathbf{b}) - \delta j_r |\delta b|^2 \right\rangle$$

**Instantaneous turbulent cascade rate $\varepsilon_L$** from single spacecraft

Taylor's hypothesis:

$\omega_{sc} = \omega_{pl} - \boldsymbol{k}\cdot\boldsymbol{v}_{sw}$ ; $\omega_{pl} << \boldsymbol{k}\cdot\boldsymbol{v}_{sw}$

Fluctuations defined as

$\mathbf{x}(t+\tau) = \mathbf{x}(\mathbf{r}_{sc} - \langle \mathbf{v}_{sw}\rangle \tau)$

$$\boxed{\varepsilon_L = \frac{3S_L(t)}{4\langle \mathbf{v}_{sw}\rangle \tau}}$$

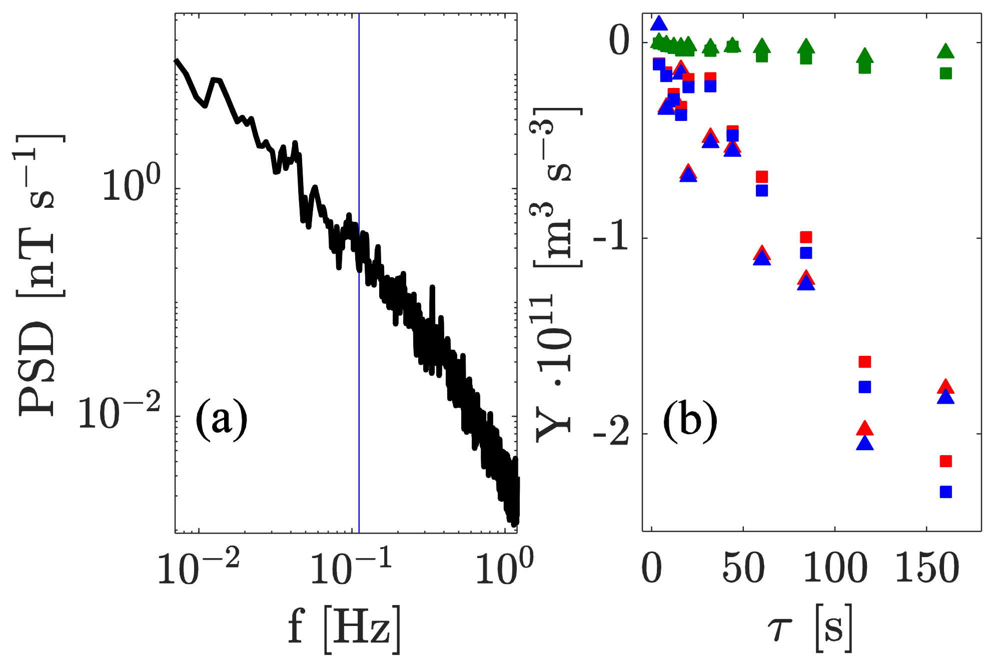

# Turbulent instantaneous energy transfer

**Question: does instantaneous energy transfer rate varies with magnetic field line topology.**

For $\boldsymbol{\varepsilon_L} > 0$ energy is transferred from large to small scales

Define: $\boldsymbol{\varepsilon}^{\circ}_{\boldsymbol{L}} \equiv \boldsymbol{\varepsilon_L} \mid D > 0$ and $\boldsymbol{\varepsilon}^{\times}_{\boldsymbol{L}} \equiv \boldsymbol{\varepsilon_L} \mid D < 0$

We compare conditional distributions p($\boldsymbol{\varepsilon}^{\circ}_{\boldsymbol{L}}$) and p($\boldsymbol{\varepsilon}^{\times}_{\boldsymbol{L}}$) using quantile-quantile plots [13]

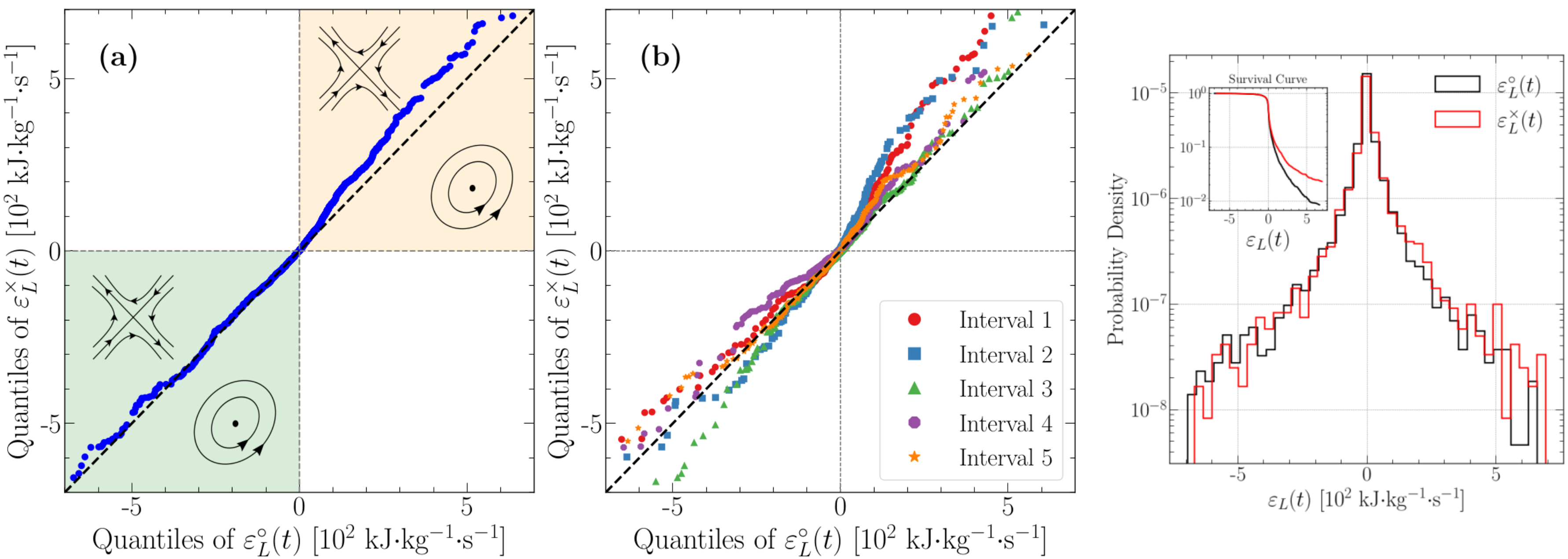


**[13]** Hnat, B et al., . (2025), Physical Review Research, **7**(4), 043058.

# Turbulent instantaneous energy transfer

**Conclusions and comments:**

- p($\varepsilon_L$ | sgn(D) ) indicates there are differences in energy transfer rate in different magnetic topologies

- In our case we find higher values of $\varepsilon_L$ in hyperbolic field line configurations, that is current sheets, or x-points

**Important notes**:

- Turbulent theory deals only with ensemble averaged moments of fluctuations, not their instantaneous values. Thus, this results is not trivially related to Yaglom's law, for example.

- Plasma velocity enters $\varepsilon_L$ estimates, and it is non-trivial problem to understand the impact of the averaged velocity on $\varepsilon_L$

# Conclusion

- Magnetic field line topology classification is a valuable tool that can assist in understanding the complex relation between local magnetic field configuration and space plasma physics.

- In the past, majority of applications borrowed heavily from hydrodynamics, but most current developments use MHD physics to understand the features/evolution of magnetic field and velocity gradient tensors

- Current efforts focus on the simulated data where spatial averaging allows us to relate magnetic field / velocity gradient tensor to the theory of MHD turbulence.